Onset of hyperon formation in neutron star matter from Brueckner theory

M. Baldo, G. F. Burgio, and H.-J. Schulze
Sezione INFN, Dipartimento di Fisica, Università di Catania, Corso Italia 57, I-95129 Catania, Italy
(Received 8 June 1998)

We determine fully self-consistent single-particle potentials and chemical potentials of nucleons and hyperons in asymmetric nuclear matter, using an extended Brueckner-Hartree-Fock formalism. We carefully analyze the onset of Σ^- and Λ formation in β stable and charge neutral matter. The role played by the three-body nucleon interaction is widely discussed. The results indicate that formation of hyperons sets in at about (2–3) times normal nuclear matter density, for all the different nucleonic equations of state that are considered. [S0556-2813(98)07512-8]

PACS number(s): 26.60.+c, 21.65.+f, 24.10.Cn

I. INTRODUCTION

The properties of neutron stars (NS) [1] depend on the knowledge of the equation of state (EOS) over a wide range of densities, i.e., from the density of iron at the star's surface to several times the density of normal nuclear matter ($\rho_0 \approx 0.17\,\mathrm{fm}^{-3}$) encountered in the core. Obviously determining the EOS over such a huge density range is a hard task. However, as far as the crust of a NS is concerned, rather reliable EOS's are available in the literature [2]. In the moderately dense regime, $\rho \approx \rho_0$, the matter consists mainly of nucleons and leptons, but at higher densities several more species of particles may appear due to the fast rise of the baryon chemical potentials with density. Among these new particles are strange baryons, namely, the Λ, Σ, and Ξ hyperons.

The hyperon thresholds are reached at densities of about (2–3) times normal nuclear density or larger, the exact value being strongly dependent on the nuclear equation of state. This dependence is traditionally investigated within relativistic mean field [3] and more phenomenological approaches [4] to the effective nucleon-nucleon and nucleon-hyperon interactions, and a wide range of possible values of the thresholds is usually obtained, according to the chosen set of parameters. It appears therefore appropriate to pin down as accurately as possible the hyperon onset densities within a microscopic, parameter-free scheme.

In this work we will examine the onset of Σ^- and Λ hyperon formation within the framework of the Brueckner-Hartree-Fock (BHF) theory. We will neglect the possible appearance of other species like pions [5] and kaons [6], as well as the possible formation of quark matter at high density [7]. These phenomena lie outside the scope of Brueckner theory that is applied here.

Due to its negative charge, the Σ^- hyperon is the first heavier baryon naively expected to appear with increasing density in the reaction $n+n \to p+\Sigma^-$ (or $n+e \to \Sigma^-$) in spite of its substantially larger mass compared to the neutral Λ hyperon ($M_{\Sigma^-}=1197\,\mathrm{MeV}, M_\Lambda = 1116\,\mathrm{MeV}$).

Quantitatively the concentrations of the various species in the dense matter are determined by the condition of charge neutrality together with the equality of chemical potentials (including rest masses) on both sides of the possible weak interaction reaction equations. In particular we have

$$\mu_e = \mu_\mu\,, \tag{1a}$$

$$\mu_n = \mu_p + \mu_e\,, \tag{1b}$$

$$2\mu_n = \mu_p + \mu_{\Sigma^-}, \tag{1c}$$

$$\mu_n = \mu_\Lambda\,, \tag{1d}$$

that are specific cases of the general formula

$$\mu = b\mu_n - q\mu_e\,, \tag{2}$$

stating that the chemical potential of any particle is a linear combination of μ_n and μ_e, weighted by the baryon number b and the electric charge number q carried by the particle.

While the chemical potentials of the leptons are simply given by the free noninteracting expressions [e.g., for the electron $\mu_e \approx (3\pi^2\rho_e)^{1/3}$ in ultrarelativistic approximation], the chemical potentials of the baryons as functions of total density and concentrations need to be determined by a microscopic calculation due to their strong interaction with the baryonic environment.

In this article we present such a microscopic investigation within an extended BHF scheme that allows us to determine the chemical potentials of the different species (n,p,Λ,Σ^-) in a fully self-consistent manner. This requires in general the knowledge of the nucleon-nucleon, nucleon-hyperon, and hyperon-hyperon strong interaction potentials in the various channels. We use in our calculation the Paris [8] and the Argonne V_{14} [9] nucleon-nucleon interactions, eventually modified by a three-body nucleon interaction (TBF). As discussed in Ref. [10], the inclusion of TBF in the nuclear matter equation of state is essential in order to get the correct saturation point. In this work, special emphasis is put on the role played by the TBF in the hyperon threshold densities.

As far as the nucleon-hyperon interaction is concerned, we use the Nijmegen soft-core [11] potentials. However, there are currently no realistic hyperon-hyperon potentials available, due to the quasicomplete lack of experimental constraints. Fortunately, for small hyperon fractions that are expected in β stable matter, and in particular for the purpose of determining the *onset* of hyperon formation that will be discussed here, the knowledge of the hyperon-hyperon interaction is not required.

II. FORMALISM

We briefly outline our formalism in the following and refer to Ref. [12] for a detailed presentation. In relation to a usual purely nucleonic BHF calculation, the problem is complicated by a coupled-channel structure: Whereas for the nucleon-nucleon interaction there are only two separate channels nn, np, or, equivalently, total isospin $T=0,1$, strong interaction transitions link the different nucleon-hyperon channels with given total charge, namely $(n\Lambda, n\Sigma^0, p\Sigma^-)$ and $(p\Lambda, p\Sigma^0, n\Sigma^+)$. There are in general $2\times 6+2$ different potentials

$$\begin{pmatrix} V_{(n\Lambda)(n\Lambda)} & V_{(n\Lambda)(n\Sigma^0)} & V_{(n\Lambda)(p\Sigma^-)} \\ V_{(n\Sigma^0)(n\Lambda)} & V_{(n\Sigma^0)(n\Sigma^0)} & V_{(n\Sigma^0)(p\Sigma^-)} \\ V_{(p\Sigma^-)(n\Lambda)} & V_{(p\Sigma^-)(n\Sigma^0)} & V_{(p\Sigma^-)(p\Sigma^-)} \end{pmatrix},$$

$$\begin{pmatrix} V_{(p\Lambda)(p\Lambda)} & V_{(p\Lambda)(p\Sigma^0)} & V_{(p\Lambda)(n\Sigma^+)} \\ V_{(p\Sigma^0)(p\Lambda)} & V_{(p\Sigma^0)(p\Sigma^0)} & V_{(p\Sigma^0)(n\Sigma^+)} \\ V_{(n\Sigma^+)(p\Lambda)} & V_{(n\Sigma^+)(p\Sigma^0)} & V_{(n\Sigma^+)(n\Sigma^+)} \end{pmatrix},$$

$$V_{(n\Sigma^-)(n\Sigma^-)}, \quad V_{(p\Sigma^+)(p\Sigma^+)}. \tag{3}$$

Based on these potentials, the various G matrices are evaluated by solving numerically the Bethe-Goldstone equation [13], written schematically [the indices a,b,c indicate nucleon-hyperon pairs (NY) as above],

$$G_{ab}[W]=V_{ab}+\sum_c \sum_{p,p'} V_{ac}|pp'\rangle \frac{Q_c}{W-E_c+i\epsilon}\langle pp'|G_{cb}[W] \tag{4}$$

with the angle-averaged Pauli operator Q and energy E of a nucleon-hyperon pair:

$$E_{(NY)}=\frac{k_N^2}{2m_N}+\frac{k_Y^2}{2m_Y}+\mathrm{Re}\,U_N(k_N)+\mathrm{Re}\,U_Y(k_Y)+m_N+m_Y. \tag{5}$$

The hyperon single-particle potentials are given by

$$U_Y(k)=\sum_{N=n,p} U_Y^{(N)}(k)$$

$$=\sum_{N=n,p}\sum_{k'<k_F^{(N)}} \langle kk'|G_{(NY)(NY)}[E_{(NY)}(k,k')]|kk'\rangle \tag{6}$$

and have separate contributions due to the neutrons and protons in the environment. The previous equations define the BHF scheme with the continuous choice of the single-particle energies. Due to the occurrence of U_N and U_Y in Eq. (5), the set of equations (4)–(6), together with the appropriate ones for the nucleons, constitutes a coupled system that has to be solved in a self-consistent manner. Currently we retain only one approximation in order to reduce the extensive computing time, namely we assume that the single-particle potentials of the three types of Σ hyperons appearing in the energy denominator of Eq. (4) are all equal. This allows one to compute the Λ and Σ^- single-particle potentials without extending the scheme to Σ^0 and Σ^+.

The total nonrelativistic energy density of hyperon-free asymmetric nuclear matter, ϵ, and the total binding energy per baryon, B/A, can be evaluated from the nucleon single-particle potentials:

$$\epsilon=\sum_{N=n,p}\frac{1}{\pi^2}\int_0^{k_F^{(N)}} dk\,k^2\left(\frac{k^2}{2m_N}+\frac{1}{2}U_N(k)\right), \tag{7}$$

$$\frac{B}{A}=\frac{\epsilon}{\rho_n+\rho_p}. \tag{8}$$

They depend on the total density of the system, $\rho=\rho_n+\rho_p$, and on the proton fraction, $x=\rho_p/\rho$.

The knowledge of the total energy as a function of total density and concentrations allows one to compute the chemical potentials of the various baryons that are required for the determination of the equilibrium composition of β stable matter. The neutron and proton chemical potentials in asymmetric matter are given by

$$\mu_n(\rho,x)=\frac{\partial\epsilon}{\partial\rho_n}=\frac{B}{A}+\left(\rho\frac{\partial}{\partial\rho}-x\frac{\partial}{\partial x}\right)\frac{B}{A}, \tag{9a}$$

$$\mu_p(\rho,x)=\frac{\partial\epsilon}{\partial\rho_p}=\frac{B}{A}+\left(\rho\frac{\partial}{\partial\rho}+(1-x)\frac{\partial}{\partial x}\right)\frac{B}{A}. \tag{9b}$$

As is well known [13,14], in Brueckner theory the following relation holds between the chemical potential μ of a species and its Fermi energy $e_F=k_F^2/2m+U(k_F)$, as determined from the single-particle potential:

$$\mu=e_F+U_2(k_F)+\cdots, \tag{10}$$

where the higher order terms represent the so-called rearrangement contributions to the single-particle potential. They were recently calculated for pure neutron matter and found to be rather small [15]. In particular it is worth noting here that in pure neutron matter the second order (in the hole line expansion) contribution U_2 vanishes for all species different from the neutron, in particular for the proton and the hyperons. [This is so since U_2 represents the conversion of a (neutron) hole state into a particle state.] This fact allows one to reliably approximate the hyperon chemical potentials by their Fermi energies.

Furthermore, knowing the chemical potentials, the proton fraction x in hyperon-free matter is obtained by solving the relevant equations for chemical equilibrium and charge neutrality,

$$\mu_e=\mu_\mu=\mu_n-\mu_p, \tag{11a}$$

$$x=x_e+x_\mu. \tag{11b}$$

Equations (11a) and (11b) form a system of three equations in the three unknown variables x, x_e, and x_μ, which can be solved numerically. In practice, the solution is uniquely determined by the quantity

$$[\mu_n-\mu_p](\rho,x)=-\frac{\partial}{\partial x}\frac{B}{A}(\rho,x). \tag{12}$$

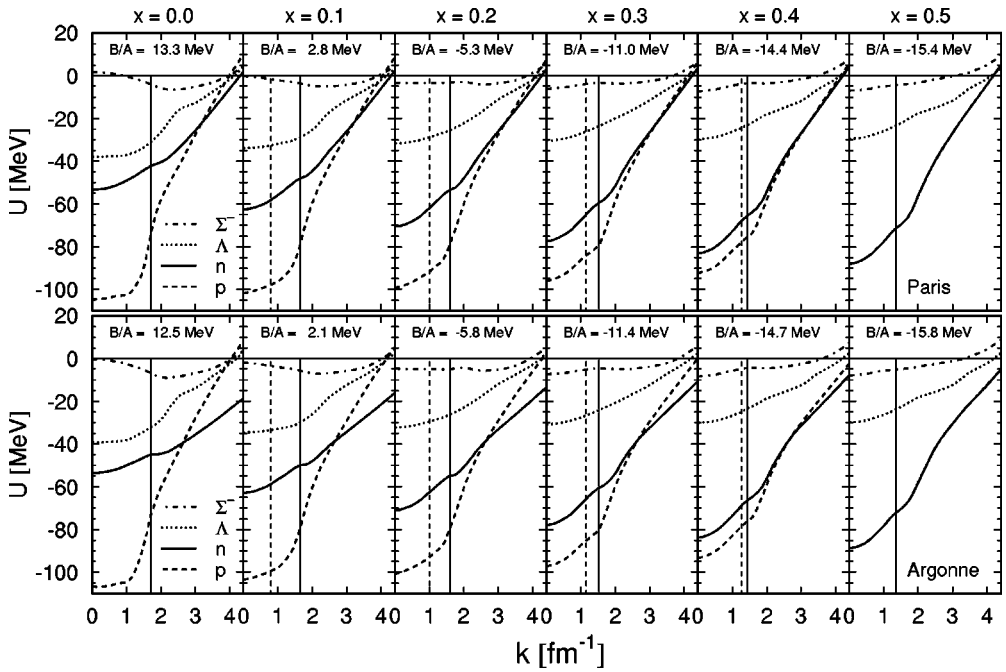

FIG. 1. Nucleon (n,p) and hyperon (Σ^-,Λ) single-particle potentials in asymmetric nuclear matter of normal density $\rho_0=0.17\ \mathrm{fm}^{-3}$ and varying proton fraction $x=0.0,0.5(0.1)$ (from left to right). The vertical lines denote the positions of the neutron (solid line) and proton (dashed line) Fermi momenta. Results obtained with the Paris (top row) and the Argonne V_{14} (bottom row) nucleon-nucleon potentials are compared.

It turns out that in the BHF approximation the binding energy per nucleon in asymmetric matter depends to a good approximation quadratically on the asymmetry parameter $\beta=1-2x$ (*parabolic approximation*) [16], i.e.,

$$\frac{B}{A}(\rho,\beta)\approx\frac{B}{A}(\rho,\beta=0)+\beta^2E_{\mathrm{sym}}(\rho), \tag{13}$$

where the so-called symmetry energy E_{sym} can then be expressed in terms of the difference of the energy per particle between pure neutron $(\beta=1)$ and symmetric $(\beta=0)$ matter:

$$E_{\mathrm{sym}}(\rho)=-\frac{1}{4}\frac{\partial}{\partial x}\frac{B}{A}(\rho,x=0) \tag{14}$$

$$\approx\frac{B}{A}(\rho,\beta=1)-\frac{B}{A}(\rho,\beta=0). \tag{15}$$

The composition of neutron star matter is therefore dependent on the nuclear symmetry energy. This quantity strongly affects the onset of hyperon formation, as well as other processes like the neutron star cooling rates [17].

In the parabolic approximation, Eq. (13), one obtains for the individual chemical potentials

$$\mu_{p,n}(\rho,\beta)=\mu_N(\rho,0)+\beta^2\rho\frac{\partial}{\partial\rho}E_{\mathrm{sym}}(\rho)-(\beta^2\pm2\beta)E_{\mathrm{sym}}(\rho) \tag{16}$$

(+ for p, − for n), where $\mu_N(\rho,0)$ is the chemical potential of a nucleon in symmetric matter. In particular Eq. (12) reduces to

$$[\mu_n-\mu_p](\rho,\beta)=4\beta E_{\mathrm{sym}}(\rho). \tag{17}$$

III. RESULTS AND DISCUSSION

A. Asymmetric nuclear matter

We come now to the presentation of our results. We begin in Fig. 1 with the display of the single-particle potentials (real parts) of neutrons, protons, Λ, and Σ^- hyperons in asymmetric nuclear matter of normal nuclear density $\rho=\rho_0$ and varying proton fraction $x=\rho_p/\rho$. The calculations have been performed with either the Paris (upper panel) or the Argonne V_{14} (lower panel) nucleon-nucleon potential. We see that for pure neutron matter $(x=0)$ the proton mean field $U(k=0)$ is much deeper $(\approx-105\ \mathrm{MeV})$ than the one of the neutron $(\approx-55\ \mathrm{MeV})$, due to the strong attraction in the $^3SD_1$ channel of the proton-neutron interaction. With increasing proton fraction the two curves approach each other until they coincide for the case of symmetric nuclear matter $(x=0.5)$.

The hyperon single-particle potentials are in general weaker than those of the nucleons due to the weaker nucleon-hyperon interaction. The lambda mean field varies from about −40 MeV in pure neutron matter to about −30 MeV in symmetric matter. Since the lambda is an isoscalar particle, this variation is exclusively due to the different intermediate states in the Bethe-Goldstone equation; it does not occur in a simple mean-field treatment. The predicted binding of lambda hyperons in symmetric nuclear matter is in good agreement with experimental data on Λ hypernuclei [18]. The Σ^- instead is rather weakly bound with a depth of the mean field close to zero. There is a slight variation of the shape of the Σ^- single-particle potential with the proton fraction. Here the experimental situation regarding sigma hypernuclei is still quite uncertain [19]. The predicted fairly small attraction of the sigma in nuclear matter (about −7

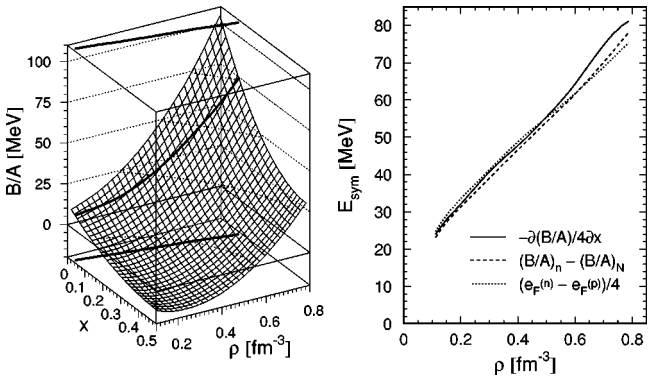

FIG. 2. Left side: Binding energy per nucleon of asymmetric nuclear matter as a function of nucleon density $\rho=\rho_n+\rho_p$ and proton fraction $x=\rho_p/\rho$. The projected curve in the plot is the line of β stability as determined from Eqs. (11a) and (11b). Right side: Nuclear symmetry energy determined by different methods. The results are obtained with the Paris potential.

MeV) seems at least not in contradiction with recent experimental data.

Regarding the differences between the two nucleon-nucleon potentials used, we find that the hyperon single-particle potentials are nearly unaffected by their choice, since the only influence is indirect via the neutron or proton single-particle potentials in the intermediate states of the Bethe-Goldstone equation, Eq. (4). These are more repulsive (in particular U_n) with the Paris potential at high momenta.

In Fig. 2 we show on the left-hand side the binding energy per nucleon, B/A, as a function of density ρ and proton fraction x, as obtained with the Paris potential. We observe that it decreases monotonically with the proton fraction for a fixed density. As mentioned before, the parabolic approximation Eq. (13) is well fulfilled. The corresponding nucleonic symmetry energy in neutron matter, $E_{\rm sym}(\rho)$, is displayed on the right hand side of the figure. It increases nearly linearly with density. We compare in the figure the result according to the definition Eq. (14), with the approximate ways (a) due to the parabolic approximation Eq. (15), and (b) from the Fermi energies, Eqs. (10) and (12), neglecting rearrangement terms. As can be seen, and discussed in the previous section, all three methods agree surprisingly well over the whole range of neutron density. The predicted value at normal density, $E_{\rm sym}(\rho_0)\approx 29\,$MeV, is in good agreement with the empirical one ($\approx$32 MeV).

With these results, we can determine the proton fraction $x(\rho)$ in β stable and charge neutral matter according to Eqs. (11a) and (11b). The resulting line of β stability, $[\rho,x(\rho)]$, is displayed on the left-hand side of Fig. 2. We notice that the proton fraction increases with the baryon density, but does not reach the critical value of about 15% needed for the occurrence of direct Urca processes [17], which are responsible for a fast neutron star cooling. In a previous work [10] we have seen that this critical value can be reached if TBF are included in the equation of state.

B. Onset of hyperon formation

We proceed now to the determination of the Σ^- and Λ threshold densities in the β stable and charge neutral matter.

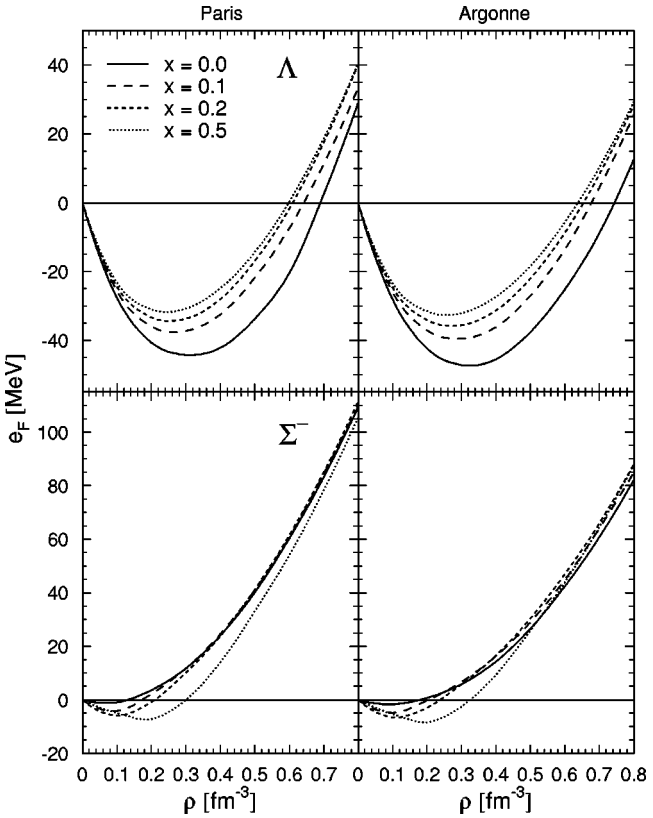

FIG. 3. The Fermi energies of Λ (top panels) and Σ^- (bottom panels) hyperons in asymmetric nuclear matter as functions of the total nucleon density ρ for different proton fractions x. The results were obtained with the Paris (left) or the Argonne V_{14} (right) nucleon-nucleon potentials.

These are determined by the vanishing along the line of β stability of the following quantities:

$$[2\mu_n-\mu_p-\mu_{\Sigma^-}](\rho,x), \tag{18a}$$

$$[\mu_n-\mu_\Lambda](\rho,x). \tag{18b}$$

These equations have to be considered together with Eqs. (11a) and (11b). The latter must be modified to include the hyperon charge, namely $x=x_e+x_\mu+x_{\Sigma^-}$. In total, one gets a closed system of five equations in the five unknown concentrations. Note, however, that since we use in these equations the chemical potentials determined in hyperon-free nuclear matter, the extracted Λ onset point is an approximate one, because for its precise determination all the chemical potentials at finite Σ^- fraction would be required. The Σ^- onset point is exact, of course, since at this stage there are no other hyperons present in the medium.

At the onset, the hyperon chemical potentials are simply given by $m_Y+U_Y(k=0)$, being m_Y the hyperon mass and U_Y the hyperon single-particle potentials, which are obtained within our BHF calculation. The single-particle depths $U_Y(k=0)$, $Y=\Sigma^-,\Lambda$ are shown in Fig. 3 as functions of the nucleon density ρ for different proton fractions. We find that the Σ^- is very weakly bound at low densities, whereas the Λ hyperon is strongly attracted in the nucleonic medium up to densities $\rho\approx 0.6\ \mathrm{fm}^{-3}$. Ultimately, with increasing density, the repulsive short-range part of the nucleon-hyperon inter-

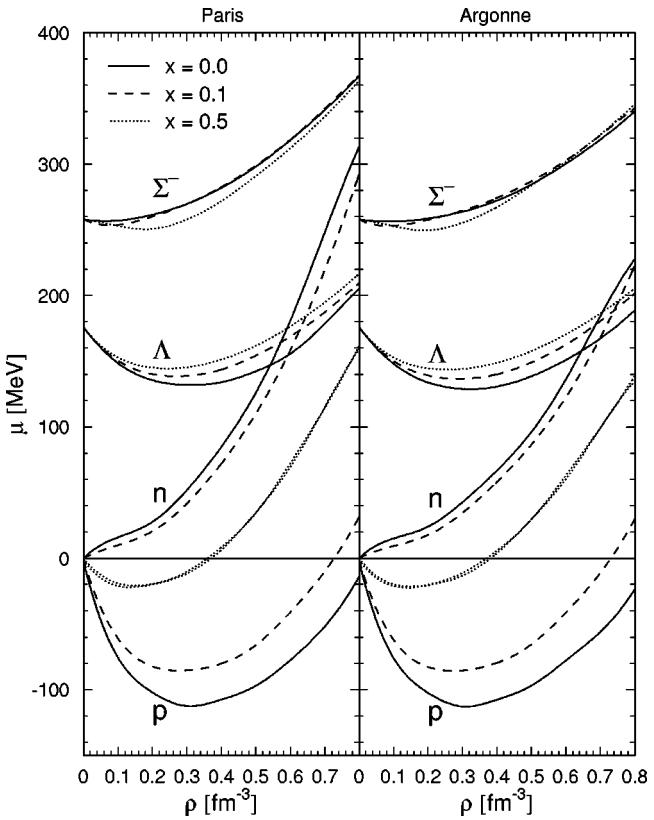

FIG. 4. Chemical potentials of nucleons (n,p) and hyperons (Λ,Σ^-) in asymmetric nuclear matter as functions of the total nucleon density ρ for different proton fractions x. Results with the Paris (left side) and the Argonne V_{14} (right side) potentials are compared.

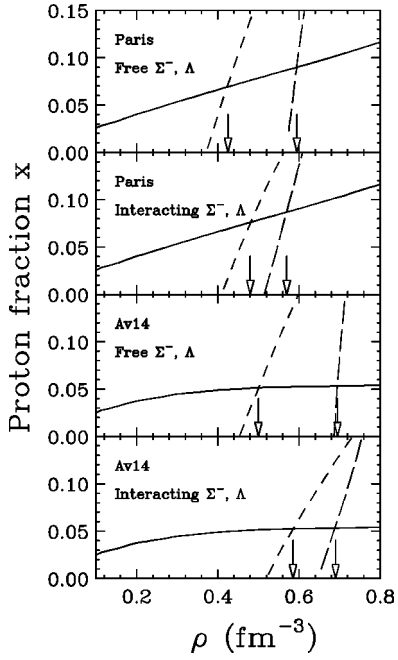

FIG. 5. The onset of Σ^- and Λ hyperon formation in the extended BHF scheme. The solid line denotes the proton fraction $x(\rho)$ in β stable and charge neutral matter. The dashed lines denote the occurrence of chemical equilibrium for Σ^- (short dashes) and Λ (long dashes) formation, according to Eqs. (18a) and (18b). The arrows indicate the onset densities of Σ^- and Λ. The different panels compare the results obtained with the Paris or Argonne nucleon-nucleon potentials, and assuming free or interacting hyperons.

action becomes dominant and forces the single-particle potentials to rise steeply with density. Concerning the dependence of the hyperon mean fields on the proton fraction, we find only moderate effects, in particular for the Σ^-. The Λ is slightly stronger bound in pure neutron matter than in symmetric matter. Since the Λ is an isoscalar particle, this effect is entirely due to the variation of the intermediate states in the Bethe-Goldstone equation with proton fraction. On the contrary, for the isovector Σ^- one could expect a stronger variation; instead, its mean field is nearly independent of the proton fraction. In this sense our numerical results are contrary to the naive expectations. The dependence of the results on the nucleon-nucleon interaction is only noticeable at high densities, where the more repulsive character of the Paris potential renders (indirectly) also the hyperon mean fields more repulsive.

The complete set of chemical potentials that are necessary to compute Eqs. (18a) and (18b) is shown in Fig. 4, taking into account the relevant differences of the rest masses $m - m_n$. We see that, compared to these mass differences, the medium effects on the hyperons, in particular the dependence on the proton fraction, are relatively small. In pure neutron matter the neutron is strongly repulsed (significantly more with the Paris than with the Argonne potential at high density), whereas the proton is substantially bound over the whole density range displayed.

Since in particular for the Σ^- we find only small medium effects at the relevant densities, it is worth comparing in the following the exact results for the hyperon onset with an approximate treatment that assumes noninteracting hyperons $(U_Y=0)$. The complete set of results is shown in Fig. 5. There we display the line of β stability [i.e., the actual proton fraction $x(\rho)$] together with the contour lines representing the zeros of Eqs. (18a) and (18b) in asymmetric nuclear matter, respectively. The intersections of the two types of curves determine the onset points (baryon density and proton fraction) of the hyperons. Results with and without nucleon-hyperon interaction, and both Paris and Argonne nucleon-nucleon potentials are compared.

As general features we note that, due to its negative charge, the Σ^- hyperon appears always before the Λ. Also, the hyperon thresholds with the Paris potential are lower than with the Argonne, due to the more repulsive character (larger neutron chemical potentials, see Fig. 4) of the former at high densities. Compared to noninteracting hyperons, in the proper calculation the onset points of Σ^- and Λ are shifted closer together, since the Σ^- mean field is repulsive, and the Λ mean field attractive at the relevant densities (see Fig. 3). In summary, in all cases the onset of the two types of hyperons takes place within the density range $\rho \approx 0.4 \ldots 0.7$ fm^{-3}.

However, one should note that the above considerations can be only qualitative, since the equations of state derived within the BHF scheme are unrealistic, being the saturation point of nuclear matter not correctly reproduced. This can be overcome by introducing three-body forces [10], which is widely discussed in the next paragraph.

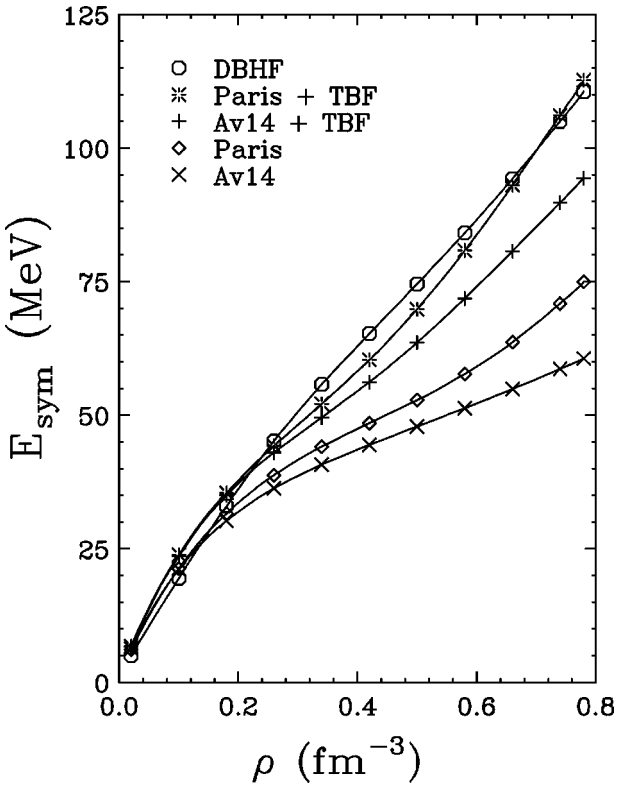

FIG. 6. Nucleonic symmetry energies determined by various theoretical models.

C. Inclusion of three-body forces

Nonrelativistic calculations, based on purely two-body interactions, fail to reproduce the correct saturation point of symmetric nuclear matter [20]. This well known deficiency is commonly corrected by introducing three-body forces (TBF), for which a complete theory is not available so far. A realistic model for nuclear TBF is the so-called Urbana model [21], which consists of an attractive term due to two-pion exchange with excitation of an intermediate Δ resonance, and a repulsive phenomenological central term. We introduced the same Urbana three-nucleon model within the BHF approach (for more details see Ref. [10]). In our approach the TBF is reduced to an effective two-body force by averaging on the position of the third particle, assuming that the probability of having two particles at a given distance is reduced according to the two-body correlation function. Therefore the resulting effective two-body force is density dependent. The corresponding EOS satisfies several requirements: (i) it reproduces correctly the nuclear matter saturation point [10]; (ii) the incompressibility at saturation is compatible with values extracted from phenomenology [22]; (iii) the symmetry energy is compatible with nuclear phenomenology; (iv) the speed of sound does not exceed the speed of light (causality condition).

Figure 6 shows the values of the symmetry energy for the different EOS's that we consider, namely the nonrelativistic Brueckner calculations with the Paris and the Argonne V_{14} potentials with and without three-body forces. For comparison, we report also the symmetry energy of a recent calculation performed with a Dirac-Brueckner (DBHF) model [23], but with the Bonn-A potential.

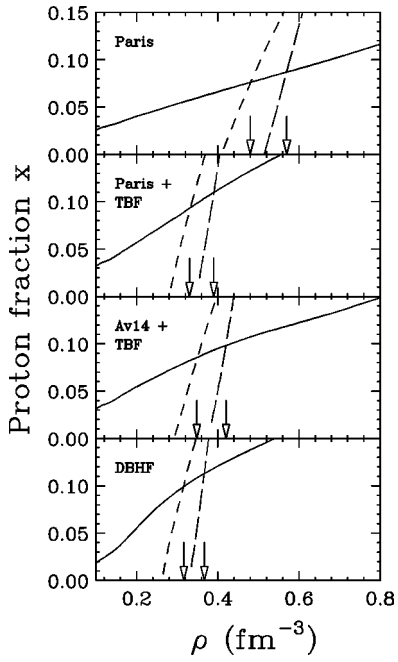

FIG. 7. The onset of Σ^- and Λ hyperon formation in different models. The notation is as in Fig. 5.

In the low density region ($\rho \lesssim 0.3\,\mathrm{fm}^{-3}$), both BHF+TBF symmetry energies and DBHF calculations are very similar, whereas at higher densities the DBHF is slightly stiffer. The discrepancy between the nonrelativistic and relativistic calculation can be easily understood by noticing that the DBHF treatment is equivalent [24] to introducing in the nonrelativistic BHF the three-body force corresponding to the excitation of a nucleon-antinucleon pair, the so-called Z-diagram [25], which is repulsive at all densities. On the contrary, in the BHF treatment both attractive and repulsive three-body forces are introduced, and therefore a softer EOS is expected.

Recently, a detailed comparison of the symmetry energies predicted by several ''modern'' nucleon-nucleon potentials was carried out [26]. The results show a good agreement of all calculations, very similar to the results with the Paris potential reported here, whereas the Argonne V_{14} predicts significantly smaller values than all other potentials. In this sense we consider our results with the Paris potential more reliable than those with the Argonne V_{14}. Coincidentally the Paris+TBF results agree very well with the DBHF over the whole range of densities.

We can proceed now to the discussion of the onset of hyperon formation when TBF are included in the equation of state. In Fig. 7 we present the results for three realistic equations of state, namely Paris+TBF, Argonne+TBF, and DBHF. For comparison, also the previous results obtained with the Paris potential and with only two-body forces are repeated in the first panel. In all these calculations the nucleon-hyperon interaction is included. We expect that the threshold densities will be lower than in the case without TBF because of the increased stiffness of the equation of state. This is indeed the case. It is gratifying to see that in spite of the variances in the predicted symmetry energies, the hyperon onset points with the different methods and potentials agree very well now. In all cases the onset of both Σ^-

and Λ hyperons takes place in the interval $\rho \approx 0.3 \ldots 0.4\,\mathrm{fm}^{-3}$.

We finally remark that now in both relativistic and nonrelativistic Brueckner-type calculations, the proton fraction x can exceed the ''critical'' value $x_{\mathrm{Urca}} \approx (11-15)\%$ needed for the occurrence of direct Urca processes [17].

IV. SUMMARY AND CONCLUSIONS

In conclusion, the knowledge of realistic nucleon-nucleon and nucleon-hyperon potentials allows the determination of a microscopic equation of state for asymmetric nuclear matter including small hyperon fractions within a self-consistent Brueckner-Hartree-Fock scheme. In this article we studied in detail the onset densities of the Σ^- and Λ hyperons. Our final results indicate that regardless of the method (nonrelativistic BHF+TBF or DBHF) and the nucleon-nucleon potentials used, the onset of the hyperons occurs at relatively low nucleonic density of about twice nuclear matter density, $\rho \approx 0.3 \ldots 0.4\,\mathrm{fm}^{-3}$.

Our results, based on a microscopic treatment of the nucleon-nucleon correlations, are in close agreement with the relativistic mean field predictions of Refs. [3]. This can be considered as a further evidence that the accurate reproduction of the nuclear saturation point is one of the key requirements which determine the thresholds of hyperon onset. Furthermore, our results provide strong restrictions on the possible phenomenological nucleon-nucleon and nucleon-hyperon effective interactions, often employed to study nuclear matter with strangeness content [4]. This shows that a microscopic treatment is required for a reliable and accurate prediction.

In the density range $\rho \approx 0.3 \ldots 0.4\,\mathrm{fm}^{-3}$ one can still expect the BHF approximation, and therefore our predictions, to be reasonably accurate, in particular for neutron matter, where the hole-line expansion appears to converge quite well [15,27]. Within the BHF framework, the biggest problem for the moment is the lack of quantitative knowledge regarding the hyperon-hyperon interactions, that might hopefully be remedied by the proposed new experiments on hypernuclear physics [28]. In that case we will be able to extract a fully microscopic equation of state for hypernuclear matter with arbitrary strangeness fraction. Furthermore, in this work we used only one nucleon-hyperon interaction, the Nijmegen soft-core model. Also here the availability of fresh experimental data should lead to the improvement of existing and the construction of new competing potentials. Nevertheless, it should be noted that due to the weaker strength of the nucleon-hyperon interaction compared to the nucleon-nucleon one, and the lower partial densities of hyperons compared to nucleons, the equation of state is still most strongly affected by the *nucleonic* properties of the dense medium. It seems, therefore, that once the correct nuclear saturation point is reproduced, the density of hyperon onset is well determined within a narrow range.

We have assumed in this work that the neutron star matter is composed exclusively of nucleons, leptons, and hyperons, and have neglected any other components (pions, kaons, quarks) that might as well appear with rising density, but do not fit into the framework of Brueckner theory. Clearly, however, with the low hyperon onset densities predicted here, the appearance of other species will be delayed or entirely impeded by the presence of hyperons.

In another publication we will study these problems and perform detailed calculations of neutron star properties based on our equations of state including hyperons.

[1] A. G. W. Cameron, Astrophys. J. **130**, 884 (1959); V. A. Ambartsumyan and G. S. Saakyan, Sov. Astron. **4**, 187 (1960); V. R. Pandharipande, Nucl. Phys. **A178**, 123 (1971); H. A. Bethe and M. B. Johnson, *ibid.* **A230**, 1 (1974); N. K. Glendenning, Z. Phys. A **326**, 57 (1987); Nucl. Phys. **A493**, 521 (1989); G. Baym, *ibid.* **A590**, 233c (1995).

[2] R. Feynman, F. Metropolis, and E. Teller, Phys. Rev. **75**, 1561 (1949); G. Baym, C. Pethick, and D. Sutherland, Astrophys. J. **170**, 299 (1971); J. W. Negele and D. Vautherin, Nucl. Phys. **A207**, 298 (1973).

[3] N. K. Glendenning, Phys. Lett. **114B**, 392 (1982); Astrophys. J. **293**, 470 (1985); N. K. Glendenning and S. A. Moszkowski, Phys. Rev. Lett. **67**, 2414 (1991); R. Knorren, M. Prakash, and P. J. Ellis, Phys. Rev. C **52**, 3470 (1995); J. Schaffner and I. N. Mishustin, *ibid.* **53**, 1416 (1996); M. Prakash, I. Bombaci, M. Prakash, P. J. Ellis, J. M. Lattimer, and R. Knorren, Phys. Rep. **280**, 1 (1997).

[4] S. Balberg and A. Gal, Nucl. Phys. **A625**, 435 (1997).

[5] G. E. Brown and W. Weise, Phys. Rep. **27**, 1 (1976); A. Akmal and V. R. Pandharipande, Phys. Rev. C **56**, 2261 (1997).

[6] V. R. Pandharipande, C. J. Pethick, and V. Thorsson, Phys. Rev. Lett. **75**, 4567 (1995); G. Q. Li, C.-H. Lee, and G. E. Brown, Nucl. Phys. **A625**, 372 (1997).

[7] E. Witten, Phys. Rev. D **30**, 272 (1984); G. Baym, E. W. Kolb, L. McLerran, T. P. Walker, and R. L. Jaffe, Phys. Lett. **160B**, 181 (1985); N. K. Glendenning, Mod. Phys. Lett. A **5**, 2197 (1990).

[8] M. Lacombe, B. Loiseau, J. M. Richard, R. Vinh Mau, J. Côté, P. Pirès, and R. de Tourreil, Phys. Rev. C **21**, 861 (1980).

[9] R. B. Wiringa, R. A. Smith, and T. L. Ainsworth, Phys. Rev. C **29**, 1207 (1984).

[10] M. Baldo, I. Bombaci, and G. F. Burgio, Astron. Astrophys. **328**, 274 (1997).

[11] P. Maessen, Th. Rijken, and J. de Swart, Phys. Rev. C **40**, 2226 (1989).

[12] H.-J. Schulze, A. Lejeune, J. Cugnon, M. Baldo, and U. Lombardo, Phys. Lett. B **355**, 21 (1995); Phys. Rev. C **57**, 704 (1998).

[13] K. A. Brueckner and J. L. Gammel, Phys. Rev. **109**, 1023 (1958); J.-P. Jeukenne, A. Lejeune, and C. Mahaux, Phys. Rep., Phys. Lett. **25C**, 83 (1976).

[14] M. Baldo, I. Bombaci, G. Giansiracusa, U. Lombardo, C. Mahaux, and R. Sartor, Phys. Rev. C **41**, 1748 (1990).

[15] W. Zuo, G. Giansiracusa, U. Lombardo, N. Sandulescu, and H.-J. Schulze, Phys. Lett. B **421**, 1 (1998).

[16] A. Lejeune, P. Grangé, M. Martzolff, and J. Cugnon, Nucl.

Phys. **A453**, 189 (1986); I. Bombaci and U. Lombardo, Phys. Rev. C **44**, 1892 (1991).

[17] J. Lattimer, C. Pethick, M. Prakash, and P. Haensel, Phys. Rev. Lett. **66**, 2701 (1991).

[18] C. B. Dover and A. Gal, Prog. Part. Nucl. Phys. **12**, 171 (1984); D. J. Millener, C. B. Dover, and A. Gal, Phys. Rev. C **38**, 2700 (1988); R. E. Chrien and C. B. Dover, Annu. Rev. Nucl. Part. Sci. **39**, 113 (1989); H. Feshbach, Nucl. Phys. **A507**, 219c (1990); Y. Yamamoto and H. Bando, Prog. Theor. Phys. **83**, 254 (1990).

[19] C. B. Dover, D. J. Millener, and A. Gal, Phys. Rep. **184**, 1 (1989); C. J. Batty, E. Friedman, and A. Gal, Prog. Theor. Phys. Suppl. **117**, 227 (1994); Y. Yamamoto, T. Motoba, H. Himeno, K. Ikeda, and S. Nagata, *ibid.* **117**, 361 (1994); R. Sawafta, Nucl. Phys. **A585**, 103c (1995).

[20] F. Coester, S. Cohen, B. D. Day, and C. M. Vincent, Phys. Rev. C **1**, 769 (1970).

[21] J. Carlson, V. R. Pandharipande, and R. B. Wiringa, Nucl. Phys. **A401**, 59 (1983); R. Schiavilla, V. R. Pandharipande, and R. B. Wiringa, *ibid.* **A449**, 219 (1986).

[22] W. D. Myers and W. J. Swiatecki, Nucl. Phys. **A601**, 141 (1996).

[23] G. Q. Li, R. Machleidt, and R. Brockmann, Phys. Rev. C **45**, 2782 (1992).

[24] M. Baldo, G. Giansiracusa, U. Lombardo, I. Bombaci, and L. S. Ferreira, Nucl. Phys. **A583**, 599 (1995).

[25] G. E. Brown, W. Weise, G. Baym, and J. Speth, Comments Nucl. Part. Phys. **17**, 39 (1987).

[26] L. Engvik, M. Hjorth-Jensen, R. Machleidt, H. Müther, and A. Polls, Nucl. Phys. **A627**, 85 (1997).

[27] M. Baldo, G. F. Burgio, H. Q. Song, and F. Weber, *Proceedings of the International Workshop on Nuclear Astrophysics*, Hirschegg, Austria (GSI, Darmstadt, 1998), p. 29.

[28] J. K. Ahn *et al.*, Nucl. Phys. **A585**, 165c (1995); M. Agnello *et al.*, *ibid.* **A623**, 279c (1997); R. Sawafta, *ibid.* **A623**, 289c (1997); R. Bertini, *ibid.* **A623**, 294c (1997).